Equilibrium Studies of a Fluorescent Paclitaxel Derivative Binding to Microtubules†

Yankun Li,‡ Richard Edsall, Jr.,‡ Prakash G. Jagtap,§ David G. I. Kingston,§ and Susan Bane*,‡

Department of Chemistry, State University of New York at Binghamton, Binghamton, New York 13902, and Department of Chemistry, Virginia Polytechnic Institute and State University, Blacksburg, Virginia 24061

Received August 31, 1999; Revised Manuscript Received November 3, 1999

ABSTRACT: A fluorescent derivative of paclitaxel, 3′-*N*-*m*-aminobenzamido-3′-*N*-debenzamidopaclitaxel (N-AB-PT), has been prepared in order to probe paclitaxel−microtubule interactions. Fluorescence spectroscopy was used to quantitatively assess the association of N-AB-PT with microtubules. N-AB-PT was found equipotent with paclitaxel in promoting microtubule polymerization. Paclitaxel and N-AB-PT underwent rapid exchange with each other on microtubules assembled from GTP-, GDP-, and GMPCPP-tubulin. The equilibrium binding parameters for N-AB-PT to microtubules assembled from GTP-tubulin were derived through fluorescence titration. N-AB-PT bound to two *types* of sites on microtubules (K_{d1} = 61 ± 7.0 nM and K_{d2} = 3.3 ± 0.54 μM). The stoichiometry of each site was less than one ligand per tubulin dimer in the microtubule (n_1 = 0.81 ± 0.03 and n_2 = 0.44 ± 0.02). The binding experiments were repeated after exchanging the GTP for GDP or for GMPCPP. It was found that N-AB-PT bound to a single site on microtubules assembled from GDP-tubulin with a dissociation constant of 2.5 ± 0.29 μM, and that N-AB-PT bound to a single site on microtubules assembled from GMPCPP-tubulin with a dissociation constant of 15 ± 4.0 nM. It therefore appears that microtubules contain two types of binding sites for paclitaxel and that the binding site affinity for paclitaxel depends on the nucleotide content of tubulin. It has been established that paclitaxel binding does not inhibit GTP hydrolysis and microtubules assembled from GTP-tubulin in the presence of paclitaxel contain almost exclusively GDP at the E-site. We propose that although all the subunits of the microtubule at steady state are the same "GDP-tubulin-paclitaxel", they are formed through two paths: paclitaxel binding to a tubulin subunit before its E-site GTP hydrolysis is of high affinity, and paclitaxel binding to a tubulin subunit containing hydrolyzed GDP at its E-site is of low affinity.

Paclitaxel (**1**, Figure 1), first reported by Wani et al. in 1971 (*1*), emerged rapidly from being a laboratory curiosity in the 1970s and 1980s to a drug of major clinical importance in the 1990s. It is currently approved by the Food and Drug Administration for the treatment of breast and ovarian cancers and for AIDS-related kaposi's sarcoma and is also used or under investigation for the treatment of a wide variety of other cancers (*2*). It is presently one of the largest selling anticancer drugs in history, with annual sales by Bristol-Myers Squibb of approximately $1 billion, and its semisynthetic analogue docetaxel (Taxotere) is also in clinical use.

The bioactivity and mechanism of action of paclitaxel have been extensively investigated (*3*−*5*). Initially discovered on the basis of the antileukemic and cytotoxic activities of *Taxus brevifolia* extracts (*1*), paclitaxel itself was found to be both strongly cytotoxic to mammalian cancer cells and also antileukemic (*6*). A major breakthrough in understanding its mechanism of action at the molecular level came in 1979 with the report by Horwitz of its ability to promote the assembly of tubulin into microtubules (*7*). The binding of paclitaxel to tubulin polymers and the associated interruption of the cell cycle were thought for a long time to be its only significant mechanism of action, with apoptotic cell death following mitotic arrest by an unknown mechanism. In recent years, however, it has been increasingly clear that paclitaxel or docetaxel can bring about apoptotic cell death by other mechanisms that appear to be independent of mitotic arrest (*8*−*11*).

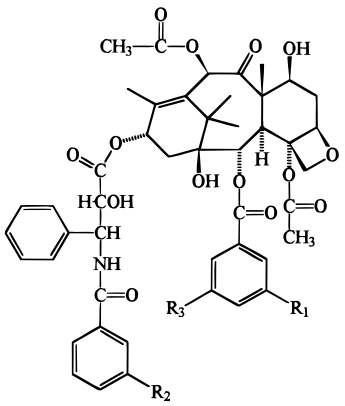

FIGURE 1: Structures of paclitaxel, N-AB-PT, and 2-DiF-PT.

The cellular effects of paclitaxel were initially ascribed to the effect of the drug on the bulk properties of microtubules. Paclitaxel induces tubulin to assemble into micro-

† This work was supported by NIH Grants CA 69571 and CA 55731.

* To whom correspondence should be addressed. Tel: (607) 777-2927. Fax: (607) 777-4478. Email: sbhastie@binghamton.edu.

‡ State University of New York at Binghamton.

§ Virginia Polytechnic Institute and State University.

10.1021/bi992044u CCC: $19.00
Published on Web 12/23/1999

tubules under conditions that are normally prohibitive (low protein concentrations and low temperatures), stabilizes microtubules against disassembly, and causes bundling of the polymers (*7*). It is now thought that the more significant property of paclitaxel is its effect on microtubule dynamics. Paclitaxel, vinblastine, cryptophycin, and colchicine have been shown to affect the dynamic properties of microtubules at concentrations far below those required to affect the bulk properties of the microtubule. The effects on dynamics also appear to be related to drug concentration. At very low concentrations of paclitaxel, catastrophic disassembly of the plus end is suppressed while assembly is maintained. At higher paclitaxel concentrations, both loss and rescue are suppressed. (*5*, *12*, *13*).

The affinity of paclitaxel for tubulin has been difficult to measure with precision. Paclitaxel associates with polymerized tubulin with a maximum stoichiometry of 1 mol of paclitaxel/mol of tubulin in the microtubule (*14*). Most investigators have found no evidence that paclitaxel binds to unassembled tubulin, although association between the unassembled protein and drug has been witnessed under certain circumstances (*15*). Measurement of the association constant of paclitaxel for microtubules is complicated by the fact that ligand binding and tubulin assembly are thermodynamically linked (*16*). Caplow et al. were able to estimate an apparent dissociation constant (15 nM) for [^{3}H]paclitaxel binding to microtubules from kinetic measurements using preassembled GMPCPP[1]-tubulin microtubules (*17*). Han et al. used a fluorescent derivative of paclitaxel, 2-AB-PT (**2**, Figure 1), to measure the dissociation constant between the paclitaxel analogue and assembled tubulin (*18*). The binding curve generated from the fluorescence data indicated the presence of more than one binding site for paclitaxel on assembled tubulin ($K_{d1} = 50$ nM, $K_{d2} = 5$ μM). The signal-to-noise ratio of the microtubule-bound ligand, however, was too low to determine definitively if both 2-AB-PT binding sites were also paclitaxel binding sites.

In this paper, another fluorescent derivative paclitaxel, N-AB-PT[1] (Figure 1), was prepared to carry out further investigations of the paclitaxel−microtubule interactions. We have found that N-AB-PT is equipotent with paclitaxel in inducing tubulin assembly in vitro, and the quantum yield of the microtubule-bound drug is significantly greater than that of 2-AB-PT bound to microtubules (*19*). This paclitaxel derivative therefore is a good candidate for quantitative analysis of the paclitaxel−microtubule association through fluorescence titrations. The results of these binding studies are presented herein.

EXPERIMENTAL PROCEDURES

Regents and Other Materials. 3′-*N*-*m*-Aminobenzamido-3′-*N*-debenzamidopaclitaxel (N-AB-PT, Figure 1) and 2-(3,5-difluorobenzoyl)paclitaxel (2-DiF-PT, Figure 1) were prepared by semisynthesis as described previously (*19*, *20*). Paclitaxel was a gift from the late Dr. Matthew Suffness (National Cancer Institute).

GTP (sodium salt, type II-S) and GDP (sodium salt, type I) were purchased from Sigma. GMPCPP [guanylyl 5′-(α,*β*-methylenediphosphonate)] was prepared from GMPCP (α,*β*-methyleneguanosine 5′-diphosphate, sodium salt, from Sigma) following the procedure described by Vulevic and Correia (*21*).

PIPES (free acid), EGTA, $MgSO_4$, and Sephadex G-50 (fine) were purchased from Sigma. The buffers used were as follows: PME buffer: 100 mM PIPES, 1 mM $MgSO_4$, 2 mM EGTA, pH 6.9; PMEG buffer: PME buffer containing 0.1 mM GTP.

Tubulin Purification and Ligand Quantification. Bovine brain tubulin, free of microtubule-associated proteins, was prepared by two cycles of temperature-dependent assembly−disassembly followed by phosphocellulose chromatography (*22*) and stored in liquid nitrogen. Prior to use, tubulin was gently thawed, centrifuged at 5000*g* for 10 min at 4 °C, and then desalted into the appropriate buffer. The concentrations of tubulin and GDP-tubulin were determined spectrophotometrically, using extinction coefficients of tubulin in PME buffer [$\epsilon_{278\ nm} = 1.23$ (mg/mL)$^{-1}$ cm^{-1} for GTP-tubulin (*23*) and $\epsilon_{278\ nm} = 1.12$ (mg/mL)$^{-1}$ cm^{-1} for GDP-tubulin (*24*)].

The concentrations of N-AB-PT and paclitaxel were also determined spectrophotometrically using extinction coefficients of N-AB-PT ($\epsilon_{320\ nm} = 2.08 \times 10^3$ M^{-1} cm^{-1} in DMSO) (*19*) and paclitaxel ($\epsilon_{228\ nm} = 2.79 \times 10^4$ M^{-1} cm^{-1} in ethanol) (*15*).

Nucleotide Exchange and Quantification. (A) Preparation of Fully Exchanged GDP-Tubulin. GDP-tubulin, in which the E-site GTP was completely replaced by GDP, was prepared as described by Seckler et al. (*25*). Tubulin (40 μM) was incubated with 5 mM GDP on ice for 30 min in PME buffer. Excess GDP and unbound GTP were removed by rapid gel filtration on Sephadex G-50 columns equilibrated with PME buffer. The nucleotide content of the GDP-tubulin was evaluated by extracting nucleotides with $HClO_4$ and determining the ratio of GTP/GDP quantitatively by HPLC (*25*).

(B) Preparation of Fully Exchanged GMPCPP-Microtubules. GDP-tubulin (5 μM) in PME buffer was incubated with 0.5 mM GMPCPP on ice for 20 min. The solution was then brought to ambient temperature for 20 min to complete polymerization. Excess GMPCPP and unbound GDP were not removed from the solution (*26*).

Polymerization Assay. Tubulin polymerizations were monitored by apparent light scattering using a Hewlett-Packard 8453 diode array spectrometer interfaced with a PC. The temperature in the thermostated multicell holder was maintained at 37 °C with a circulating water bath. The assays were performed in the kinetics mode of the instrument. Tubulin (10 μM) in PMEG buffer was equilibrated to temperature, and a base line was recorded. Assembly was initiated by adding N-AB-PT or paclitaxel to the cuvette followed by rapid mixing. The apparent absorption at 400 nm was recorded at 30 s intervals until a steady state was reached. The extent of tubulin assembly was determined from the difference in the base line and the plateau absorption values.

[1] Abbreviations: 2-AB-PT, 2-debenzoyl-2-(*m*-aminobenzoyl)paclitaxel; 2-DiF-PT, 2-(3,5-difluorobenzoyl)paclitaxel; DMSO, dimethyl sulfoxide; GDP, guanosine 5′-triphosphate; GMPCPP, guanylyl 5′-(α,*β*-methylenediphosphonate); GTP, guanosine 5′-triphosphate; HPLC, high-pressure liquid chromatography; N-AB-PT, 3′-*N*-*m*-aminobenzamido-3′-*N*-debenzamidopaclitaxel; PIPES, piperazine-*N*,*N*′-bis(2-ethanesulfonic acid); PME buffer, 50 mM PIPES, 0.5 mM $MgSO_4$, 1 mM EGTA, pH 6.9; PMEG buffer, PME buffer containing 0.1 mM GTP, pH 6.9.

Absorption Spectroscopy. Ultraviolet absorption spectra were obtained on a Hewlett-Packard 8453 diode array spectrometer at ambient temperature. The instrument was set in the standard mode. Spectral data were digitally exported to a PC for analysis.

Fluorescence Spectroscopy. Fluorescence excitation and emission spectra of N-AB-PT were obtained at ambient temperature on an SLM 48000 spectrofluorometer connected to a PC. Excitation spectra were corrected by using Rhodamine B in ethylene glycol (3 g/L) in the reference channel. Emission spectra were uncorrected. A 2 × 10 mm quartz cuvette was used for the measurements and was oriented such that the excitation beam passed through the smaller path, to eliminate or minimize any possible inner filter effect. Corresponding background spectra were recorded and digitally subtracted from the sample spectra. The apparent fluorescence of microtubules in the samples due to light scattering was negligible under experimental conditions.

The photochemical lifetime of N-AB-PT bound to microtubules was measured on the SLM 48000 using the phase modulation method with glycogen as the light scatter reference (*27*).

Binding Competition between N-AB-PT or 2-DiF-PT and Paclitaxel on Microtubules Assembled from GTP-Tubulin. Tubulin (5 μM) in PME buffer was incubated with 5 μM N-AB-PT or 2-DiF-PT and varying amounts (0−40 μM) of paclitaxel at 37 °C for 30 min. The fluorescence emission spectrum of each sample was measured (excitation wavelength = 320 nm). The amount of microtubule-bound N-AB-PT was determined by the fluorescence intensity at 420 nm. The emission of free N-AB-PT at this wavelength under the experimental conditions was negligible.

Ligand Exchange. (A) Ligand Exchange on Microtubules Assembled from GTP-Tubulin. Three samples were prepared by incubating tubulin (5 μM) in PME buffer with paclitaxel (15 μM) and N-AB-PT (15 μM) in different ways. Sample A: tubulin incubated with N-AB-PT at 37 °C for 30 min, paclitaxel added and then incubated another 30 min. Sample B: N-AB-PT and paclitaxel added at the same time, incubated at 37 °C for 30 min. Sample C: tubulin incubated with paclitaxel at 37 °C for 30 min, N-AB-PT added and then incubated another 30 min. A reference sample was prepared by incubating tubulin (5 μM) with N-AB-PT (15 μM) at 37 °C for 30 min. The fluorescence emission spectrum of each sample was measured (excitation wavelength = 320 nm). The amount of microtubule-bound N-AB-PT was determined by the fluorescence intensity at 420 nm. The fluorescence due to free N-AB-PT under the experimental conditions was negligible.

Kinetics of ligand exchange were also measured by monitoring the emission intensity at 420 nm (excitation wavelength = 320 nm) in the slow-time emission acquisition mode at 1 s intervals. The temperature was maintained at 37 °C with a circulating water bath. Tubulin (5 μM) was incubated with one taxoid (15 μM) for 30 min, and a base line was recorded. The second taxoid (15 μM) was then added followed by rapid mixing. The fluorescence emission intensity was continually monitored until a plateau was reached.

(B) Ligand Exchange on Microtubules Assembled from GDP-Tubulin and GMPCPP-Tubulin. Ligand exchange between paclitaxel and N-AB-PT bound to microtubules assembled from GDP- and GMPCPP-tubulin was measured as described above; 20 μM paclitaxel and 20 μM N-AB-PT were used with 5 μM GDP-tubulin, and 10 μM paclitaxel and 10 μM N-AB-PT were used with 5 μM GMPCPP-tubulin.

Equilibrium Binding Measurements. (A) N-AB-PT Binding to Microtubules Assembled from GTP-Tubulin. Tubulin (5 μM) in PME buffer was incubated with varying amounts of N-AB-PT (0−35 μM) at 37 °C for 30 min. The fluorescence emission spectrum of each sample was measured (excitation wavelength = 320 nm), and the emission intensity at 420 nm was recorded. The samples were then centrifuged at 90000*g* in a Beckman 42.2 Ti rotor at 23 °C for 20 min to pellet the microtubules. The supernatant of each sample was collected by careful aspiration, and the absorption and emission spectra of each sample were measured again at ambient temperature under the same instrumental conditions.

The emission intensities were converted into concentration data by dividing each emission intensity by the emission intensity per micromolar fully microtubule-bound N-AB-PT ($F_{\text{per }\mu\text{M}}$). This value was obtained by incubating N-AB-PT (5 μM) with excess tubulin (20 μM) and measuring the emission spectrum. Three identical samples were used for each determination of $F_{\text{per }\mu\text{M}}$.

The fluorescence data were fit to the binding equation:

$$r = \sum\{n_i[\text{N-AB-PT}]_{\text{free}}/(K_{\text{d},i} + [\text{N-AB-PT}]_{\text{free}})\}$$

where r denotes the binding function ($[\text{N-AB-PT}]_{\text{bound}}/[\text{MT}]_{\text{total}}$). $[\text{N-AB-PT}]_{\text{bound}}$ and $[\text{N-AB-PT}]_{\text{free}}$ are the concentrations of microtubule-bound N-AB-PT and free N-AB-PT in each sample, respectively. $[\text{MT}]_{\text{total}}$ is the total concentration of tubulin in the form of microtubules in each sample. K_{d} is the apparent dissociation constant of each site, and n is the apparent stoichiometry for each site.

$[\text{N-AB-PT}]_{\text{bound}}$ was determined as follows: For each sample, the net fluorescence emission intensity of microtubule-bound N-AB-PT (F_{bound}) at 420 nm was obtained by subtracting the emission intensity of the supernatant (due to free ligand and background) from the emission intensity of the original solution at the same wavelength. F_{bound} was then divided by the emission intensity of per μM microtubule-bound N-AB-PT, $F_{\text{per }\mu\text{M}}$, to convert to the concentration of microtubule-bound N-AB-PT, $[\text{N-AB-PT}]_{\text{bound}}$. $[\text{N-AB-PT}]_{\text{bound}}$ was subtracted from the total concentration of N-AB-PT in each sample to obtain $[\text{N-AB-PT}]_{\text{free}}$.

$[\text{MT}]_{\text{total}}$ was obtained by subtracting the concentration of unassembled tubulin in each sample from the total tubulin concentration (5 μM). The concentration of unassembled tubulin was determined from the absorption spectrum of the supernatant using the extinction coefficient of tubulin.

The data were fit to the binding equation using the curve-fitting software (Marquardt−Levenberg algorithm) in SigmaPlot 4.0 (Jandel Scientific).

(B) N-AB-PT Binding to Microtubules Assembled from GDP-Tubulin. GDP-tubulin (5 μM) was incubated with varying amounts of paclitaxel (0−35 μM) in PME buffer at 37 °C for 30 min to ensure complete polymerization. The measurements and data analyses were performed as described above for GTP-tubulin, except that $F_{\text{per }\mu\text{M}}$ was obtained by incubating 5 μM N-AB-PT with 50 μM GDP-tubulin to ensure the complete binding of the ligand.

(C) N-AB-PT Binding to Microtubules Assembled from GMPCPP-Tubulin. Microtubules polymerized from 5 μM GMPCPP-tubulin were incubated with varying amounts of paclitaxel (0−20 μM) in PME buffer at 37 °C for 30 min to ensure complete polymerization. The measurements and data analyses were performed as described above for GTP-tubulin. The total concentration of tubulin in the form of microtubules, $[MT]_{total}$, was 5 μM for all samples.

(D) N-AB-PT Binding to Microtubules Preassembled by GTP. Tubulin (50 μM) was incubated with 1 mM GTP in PME buffer at 37 °C for 30 min. It was then diluted into PME buffer containing 0−10 μM N-AB-PT. The final concentration of tubulin in each sample was 5 μM. The samples were then incubated at 37 °C for 30 min. The measurements and data analyses were performed as describes above.

Nucleotide Content of GTP-Tubulin Microtubules Induced by N-AB-PT. Microtubules were prepared by incubating tubulin (10 μM) in PME buffer with 20 μM N-AB-PT at 37 °C for 30 min. Nucleotides were extracted from the tubulin subunits with $HClO_4$ and processed. The ratio of GTP/GDP was evaluated by HPLC as described by Seckler et al. (*25*).

Electron Microscopy. Electron micrographs were obtained using a Hitachi 7000 TEM. Samples were prepared on 200 mesh hydrophilic carbon-coated grids and then stained with 0.5% uranyl acetate solution.

RESULTS

Microtubule-Promoting Properties of N-AB-PT. Like paclitaxel, N-AB-PT induced assembly of purified tubulin into microtubules. Figure 2A shows the effect of N-AB-PT on tubulin assembly. The extent of microtubule assembly increased with increasing amounts of N-AB-PT until reaching the plateau at a molar ratio of approximately 1:1 (N-AB-PT:tubulin). Additional N-AB-PT did not seem to affect the polymer mass, suggesting that most of the tubulin dimers were incorporated into the microtubules. Control experiments done with paclitaxel under the same conditions yielded identical results (data not shown). The critical concentration for tubulin assembly, the concentration below which no microtubule assembly is observed, was also determined for N-AB-PT (Figure 2B). In the presence of 20 μM N-AB-PT, the critical concentration was 0.3 ± 0.1 μM. Again, identical experiments with paclitaxel gave the same result within experimental error. The tubulin polymers formed by N-AB-PT were confirmed to be microtubules by electron microscopy (data not shown). The effect of N-AB-PT on nucleotide hydrolysis was also examined. It was found that the nucleotide content of N-AB-PT-assembled GTP-tubulin microtubules was 1:1 (GTP:GDP). Therefore, addition of a *m*-amino group to the 3′-benzamide has no observable effect on the assembly-promoting properties of paclitaxel.

Equilibrium Binding of N-AB-PT to the Paclitaxel Site on Microtubules. The microtubule-promoting properties of N-AB-PT were determined to be due to N-AB-PT binding to the paclitaxel site on microtubules through competition experiments. We have found that microtubule binding induces a significant blue shift in the emission maximum of N-AB-PT (from 442 nm in PME buffer to 424 nm for microtubule-bound N-AB-PT) and an increase in quantum yield (from 0.12 to 0.56). Energy transfer between the protein and the drug was observed as well (*19*). Paclitaxel caused a concentration-dependent decrease in the emission intensity of microtubule-bound N-AB-PT (Figure 3). The competition experiment was repeated with 2-DiF-PT, which is about twice as potent as paclitaxel in promoting tubulin polymerization (data not shown). It is seen in Figure 3 that 2-DiF-PT was also more effective in inhibiting N-AB-PT binding to assembled tubulin. These data indicate that N-AB-PT and paclitaxel bind to the same site(s) on the microtubule.

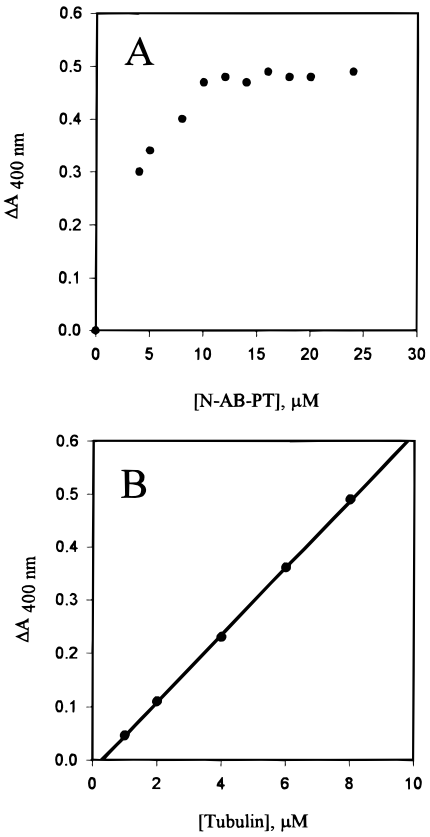

FIGURE 2: Effects of N-AB-PT on in vitro tubulin polymerization. (A) Extent of tubulin polymerization as a function of N-AB-PT concentration. Tubulin (10 μM) in PMEG buffer was polymerized by addition of varying amounts of N-AB-PT at 37 °C. The turbidity increase was monitored at 400 nm. (B) Critical tubulin concentration for microtubule polymerization in PMEG buffer in the presence of 20 μM N-AB-PT.

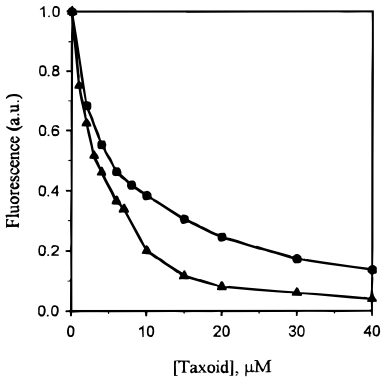

FIGURE 3: Equilibrium binding competition between taxoids on microtubules. Samples were prepared by incubating tubulin (10 μM) with 10 μM N-AB-PT and varying amounts of paclitaxel (solid circles) or 2-DiF-PT (triangles) at 37 °C for 30 min. The amount of microtubule-bound N-AB-PT was determined by the emission intensity at 420 nm (excitation wavelength = 320 nm). The emission of free N-AB-PT was negligible under the experimental conditions.

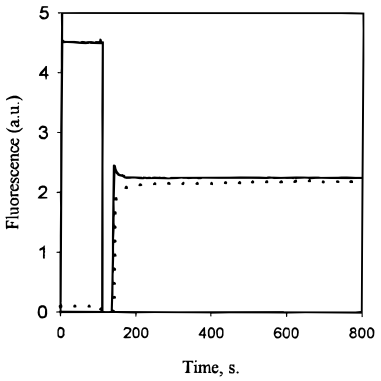

FIGURE 4: Ligand exchange observed by fluorescence of microtubule-bound N-AB-PT. Tubulin (5 μM) was incubated at 37 °C with one taxoid (15 μM) for 30 min, a base line was recorded, and the second taxoid was then added. Solid line: tubulin incubated with N-AB-PT first. Dotted line: tubulin incubated with paclitaxel first. The excitation and emission wavelengths were at 320 and 420 nm, respectively.

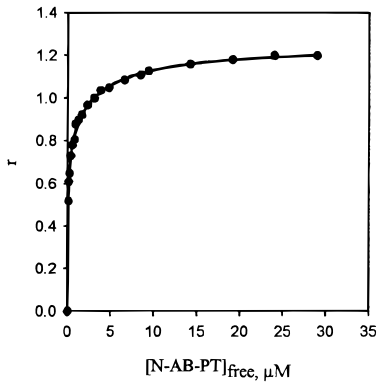

FIGURE 5: Binding of N-AB-PT to GTP-tubulin microtubules. Tubulin (5 μM) was titrated with varying amounts of N-AB-PT as described under Experimental Procedures. *r* is the binding function ($[\text{N-AB-PT}]_{bound}/[\text{microtubule}]_{total}$). The solid curve is the data fit to a double rectangular hyperbola.

Whether N-AB-PT and paclitaxel could undergo ligand exchange was evaluated. Figure 4 shows the effect of adding paclitaxel (15 μM) to a solution containing 5 μM GTP-tubulin and 15 μM N-AB-PT. The emission intensity due to polymer-bound drug immediately decreased to about 50% of its original value. When N-AB-PT (15 μM) was added to microtubules formed from 5 μM GTP-tubulin with 15 μM paclitaxel, emission at 430 nm rapidly appeared (2−3 min; dotted line, Figure 4). Adding the two ligands simultaneously produced equivalent fluorescence emission intensity. Similar experiments with GDP-tubulin and GMPCPP-tubulin gave rise to the same results. These data indicate that paclitaxel and N-AB-PT undergo rapid and reversible association with polymerized tubulin and that the two ligands have about equal affinity for the paclitaxel binding site on the microtubule.

Equilibrium Binding of N-AB-PT to Microtubules Assembled from GTP-Tubulin. Equilibrium dissociation constants for N-AB-PT binding to microtubules were measured through fluorescence titrations. Tubulin in PME buffer was titrated with varying amounts of N-AB-PT at 37 °C as described under Experimental Procedures. Briefly, varying amounts of N-AB-PT were added to GTP-tubulin at 37 °C. Samples were incubated to allow the assembly process to occur. The concentration of microtubule-bound N-AB-PT was derived from the fluorescence emission intensity. The equilibrium binding curve is shown in Figure 5. The data were best fit to a double-rectangular hyperbola, indicating that there are two types of binding sites for paclitaxel on microtubules. A Hill plot of the data showed no evidence for cooperativity, so the two types of binding sites were considered to be independent. Nonlinear regression analysis of the binding curve yielded the following parameters for the two types of binding sites (Table 1). The high-affinity site had an apparent dissociation constant of 61 nM and a stoichiometry of about 0.8 site per tubulin dimer in the microtubule. The second binding site had a 50-fold lower affinity, with an apparent dissociation constant of 3.3 μM and a stoichiometry of 0.44 site per tubulin dimer in the tubulin polymer.

The effect of preassembling the tubulin on the equilibrium binding parameters of N-AB-PT was explored. In this experiment, GTP-tubulin was incubated at 37 °C prior to the addition of N-AB-PT. Again two types of binding sites were found. The affinities of these sites are the same as those obtained from native tubulin within experimental error, and the total stoichiometry is approximately 1 (Table 1). However, the stoichiometric ratio of these two types of sites changed from 1.8:1 (higher affinity:lower affinity) to 0.7:1.

Table 1: Apparent Dissociation Constants and Stoichiometry for Paclitaxel or N-AB-PT Binding to the Paclitaxel Site on Microtubules at 37 °C

tubulin-bound nucleotide[a]	K_{d1}, μM[b]	n_1[c]	K_{d2}, μM	n_2
GTP-tubulin[d]	0.061 (0.007)[e]	0.81 (0.03)[f]	3.3 (0.54)	0.44 (0.02)[f]
GTP-tubulin, preassembled[d,g]	0.046 (0.014)	0.47 (0.03)[f]	5.3 (2.0)	0.64 (0.08)[f]
GDP-tubulin[d]	2.5 (0.29)	1.0 (0.04)	nd[h]	nd
GMPCPP-tubulin[d]	0.015 (0.004)	1.1 (0.3)	nd	nd
GMPCPP-tubulin, kinetic[i]	0.015	—	—	—

[a] Refers to the content of exchangeable GTP binding site of tubulin prior to assembly. [b] Dissociation constant at 37 °C. [c] Moles of taxoid/moles of tubulin in the polymer. [d] Binding parameters determined using N-AB-PT, as described under Experimental Procedures. [e] Standard deviations are in parentheses. [f] See footnote 2. [g] Tubulin was preassembled into microtubules by GTP prior to the addition of N-AB-PT; see text. [h] Not detected. [i] Binding parameters determined using paclitaxel and a kinetic assay, from ref *17*.

Binding of N-AB-PT to Microtubules Assembled from GDP-Tubulin or GMPCPP-Tubulin. The titration experiments were again performed using tubulin in which the E-site GTP had been completely replaced by GDP or by GMPCPP (a weakly hydrolyzable GTP analogue). It was found that N-AB-PT bound to a single site on the tubulin dimer within the microtubule on GDP-microtubules with a dissociation constant of 2.5 μM (Figure 6). Similarly, N-AB-PT was found to bind to a single site on GMPCPP-microtubules with a dissociation constant of 15 nM (Figure 7). These data are summarized in Table 1.

The microtubules formed from GTP-tubulin, GDP-tubulin, and GMPCPP-tubulin in the presence of N-AB-PT were examined by electron microscopy. Normal microtubules were observed in each case. Microtubules from GDP-tubulin were significantly longer than reference microtubules from GTP-tubulin, while GMPCPP-microtubules were much shorter yet more numerous and appeared no different in the presence

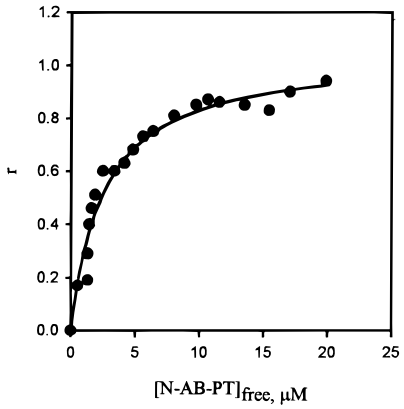

FIGURE 6: Binding of N-AB-PT to GDP-tubulin microtubules. GDP-tubulin (5 μM) was titrated with varying amounts of N-AB-PT as described under Experimental Procedures. The solid curve is the data fit to a single rectangular hyperbola.

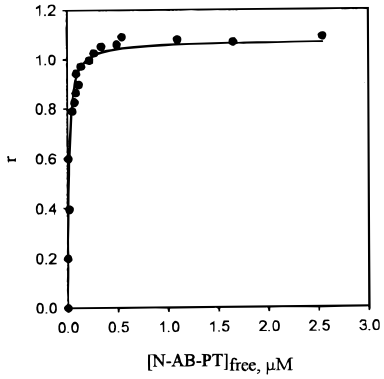

FIGURE 7: Binding of N-AB-PT to GMPCPP-tubulin microtubules. GMPCPP-tubulin (5 μM) was titrated with varying amounts of N-AB-PT as described under Experimental Procedures. The solid curve is the data fit to a single rectangular hyperbola.

or absence of N-AB-PT. These observations are in concordance with previous studies (*24*, *26*, *28*,).

Fluorescence Lifetimes of Microtubule-Bound N-AB-PT. The differences in binding affinities of N-AB-PT for different types of microtubules led us to question whether the spectroscopic properties of the microtubule-bound ligand were also different. The shape of the emission spectra of the microtubule-bound N-AB-PT appeared identical regardless of the nucleotide content of tubulin, but the emission intensities were different. For example, the fluorescence intensity of N-AB-PT bound to GDP-tubulin microtubules at the emission maximum (424 nm) was about 30% greater than that of N-AB-PT bound to GMPCPP-tubulin microtubules. Moreover, the lifetime of N-AB-PT bound to microtubules from GDP-tubulin was found to be 15% longer than that of N-AB-PT bound to GMPCPP-tubulin microtubules (15.5 $\pm$ 0.3 ns vs 13.8 $\pm$ 0.2 ns), which is consistent with the intensity differences between these two samples. The lifetime of N-AB-PT bound to GTP-tubulin microtubules was 14.1 $\pm$ 0.2 ns.

DISCUSSION

N-AB-PT, a fluorescent derivative of paclitaxel, affects in vitro tubulin assembly in manners identical to paclitaxel. Competition experiments show that the two drugs share the same binding site. The relatively large quantum yield of the microtubule-bound drug (*19*) provides a good signal-to-noise ratio for the bound species. These characteristics made N-AB-PT an excellent probe for investigating paclitaxel−microtubule interactions using fluorescence spectroscopy.

N-AB-PT is more water-soluble than most taxoids (>100 μM in water containing 4% DMSO). Low solubility of paclitaxel has been problematic in its clinical use, and derivatives with improved water solubility have been widely sought (*2*). Since N-AB-PT is equipotent with paclitaxel in receptor binding ability, investigations into the in vivo activity of this compound are warranted.

Relationships between Paclitaxel Binding, Nucleotide Content, and Tubulin Polymerization. The simplest results were obtained for N-AB-PT binding to GDP-tubulin microtubules and GMPCPP-tubulin microtubules. We found that microtubules assembled from GDP-tubulin or GMPCPP-tubulin possess a single type of paclitaxel binding site. Since these microtubules have a homogeneous nucleotide content and are devoid of dynamic instability (*24*, *29*), a uniform binding site along the microtubule lattice would be expected in both cases. It appears that the conformation features that affect the assembly properties of GMPCPP-tubulin and GDP-tubulin also affect the binding of paclitaxel to these proteins. GMPCPP-tubulin is thought to exist in a "straight" conformation, which appears to promote stronger lateral interactions between protofilaments (*30*). GMPCPP-tubulin assembles at ambient temperature without exogenous ligands into highly stable microtubules (*26*). GDP-tubulin, with a conformation that is more "curved" than GTP-tubulin (*31*), forms ring-like oligomers rather than microtubules in the absence of paclitaxel (*32*). It has been proposed that paclitaxel binding to GDP-tubulin oligomers induces a conformational change in the protein to an active, GTP-tubulin-like conformation, which will then support microtubule assembly (*14*).

Although the nucleotide content of tubulin clearly affects the overall structure of the protein (*33*), there is only a single report of the nucleotide content of the exchangeable GTP site affecting drug binding sites on the soluble tubulin heterodimer **(***34*). Our data demonstrate that the nucleotide-dependent tubulin conformation substantially affects the paclitaxel binding site on tubulin assembled into microtubules. The equilibrium constant for N-AB-PT binding to GMPCPP-tubulin microtubules is almost 170 times greater than the equilibrium constant for N-AB-PT binding to GDP-tubulin microtubules (Table 1). This difference corresponds to a difference in free energy change ($\Delta\Delta G°$) of about 3.2 kcal/mol at 37 °C. But the free energy change for taxoid binding to GDP-microtubules is linked to the elongation of the microtubule (*14*), so the affinity constant measured for N-AB-PT binding to GDP-microtubules is a function of both the overall binding and the association process. Diaz and Andreu have determined that the difference in elongation free energy between the paclitaxel-induced assembly of GTP-tubulin and GDP-tubulin is less than 1 kcal/mol. Therefore, we estimate that the binding of N-AB-PT to GMPCPP-tubulin microtubules is at least 2 kcal/mol more exothermic than the binding of the ligand to the paclitaxel site on GDP-tubulin microtubules. We speculate that the difference in affinity may be due to an altered protein conformation within the region of the paclitaxel binding site.

The association of N-AB-PT with GTP-tubulin microtubules is more complex. We find two *types* of independent binding sites for paclitaxel on the GTP-tubulin micro-

Scheme 1

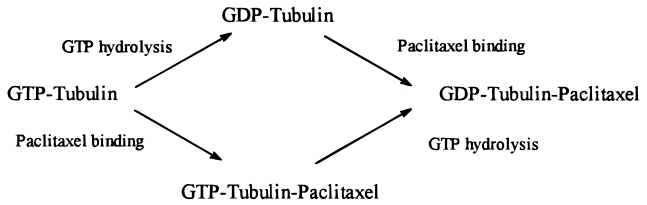

tubule: a higher affinity site with a dissociation constant in the nanomolar range, and a lower affinity site with a dissociation constant in the micromolar range. The experiment was performed using two different protocols. In the first experiment, N-AB-PT was added to GTP-tubulin prior to assembly; in the second, N-AB-PT was added to preassembled microtubules. Changing the experimental conditions in this manner changed the relative stoichiometry, but did not change the association constants within experimental error (Table 1).[2]

The maximum stoichiometry found for paclitaxel binding to microtubules is consistently 1 mol of paclitaxel/mol of assembled tubulin dimer (*14*, *35*). Yet several investigators have noted that microtubules seem to have more than one type of binding site for paclitaxel (*5*, *18*, *36*, *37*). Our equilibrium binding studies provide a quantitative explanation for these seemingly contradictory observations: microtubules assembled from GTP-tubulin have a total of 1 paclitaxel binding site per mole assembled tubulin dimer, but the nature of the binding site is not uniform within the GTP-tubulin microtubule. We propose that the two types of N-AB-PT binding sites on GTP-tubulin microtubules are the result of drug binding to different conformations of tubulin in the microtubule, and that these two different tubulin conformations are caused by the nucleotide bound to the exchangeable GTP site.

Our equilibrium data indicated that a substantial fraction of tubulin in microtubules assembled from GTP-tubulin was in the "straight" conformation (Table 1). Analysis of the nucleotide content of these microtubule showed a 1:1 ratio of GTP:GDP, which is also observed for paclitaxel-polymerized tubulin (*36*). It therefore appeared that the equilibrium data were at odds with the GTP hydrolysis data.

We explain the apparent incongruity by considering the sequence of three events: GTP-tubulin binding to the end of a microtubule, GTP hydrolysis in the polymer, and paclitaxel binding to microtubule. From a macroscopic standpoint, these events take place simultaneously. GTP-tubulin microtubules at steady state fully saturated with paclitaxel are composed almost exclusively of "GDP-tubulin-paclitaxel" subunits, which each contain one GDP at the E-site and one molecule of paclitaxel. However, such a "GDP-tubulin-paclitaxel" subunit can be obtained through two different paths (Scheme 1). A tubulin dimer in the active GTP conformation may have two fates shortly after it is incorporated into the end of a microtubule. In the first route, paclitaxel binds to the GTP-tubulin subunit on the end of the microtubule, before hydrolysis of the E-site GTP hydrolysis. Following the second path, the E-site GTP of this subunit hydrolyzes first; the subsequent paclitaxel binding to this GDP subunit can take place either before or after its association with a new GTP-tubulin dimer. The relative stoichiometry of the higher and lower affinity sites can therefore change depending on experimental conditions. In our case, adding N-AB-PT to preassembled GTP-tubulin microtubules resulted in more lower affinity sites than adding the ligand prior to assembly. This result fits our model: a larger proportion of tubulin in the microtubule is expected to be in the GDP-tubulin conformation in the preassembled sample. Tubulin in the GTP conformation will continue to bind to the microtubule ends, which may then bind paclitaxel. Since microtubules fully liganded with paclitaxel are not dynamic (*24*, *29*), variations in the stoichiometric ratio are expected.

This hypothesis has a number of implications in our understanding of the interactions between paclitaxel and tubulin. We found physical evidence that the ends of the microtubule differ from the walls of the microtubule with respect to paclitaxel binding, and that the origin of these differences is the nucleotide-engendered conformational state of the protein. The in vitro assays of drug potencies using purified tubulin are routinely performed with GTP-tubulin. Since N-AB-PT binding to the end of the microtubule is mimicked by N-AB-PT binding to GMPCPP-tubulin microtubules, the affinities of paclitaxel-like drugs for GMPCPP-tubulin microtubules may be more indicative of their antitumor activity than their activities on GTP-tubulin.

Other observations from the literature also support our model. For example, Arnal and Wade (*38*) found that the moire repeat length L_N, which can provide information about the length of tubulin within the polymer, is significantly increased by paclitaxel *only if* tubulin is assembled in the presence of paclitaxel. Addition of paclitaxel during assembly yields polymers with L_N values just slightly larger than those of reference microtubules. This result is expected based on our equilibrium data: addition of N-AB-PT to preassembled microtubules gave a lower ratio of high:low-affinity binding site stoichiometry than adding the drug during assembly.

Stoichiometry of N-AB-PT Binding to GTP-Tubulin Microtubules. The stoichiometry of taxoids binding to microtubules has been meticulously measured to be one ligand per tubulin subunit (*14*, *35*). The same results were also obtained in our binding studies when GDP-tubulin or GMPCPP-tubulin was used. The total stoichiometry of N-AB-PT binding to GTP-tubulin, however, was between 1.10 and 1.25 $\pm$ 0.05 mol of ligand per assembled tubulin dimer. We therefore set out to find the reason(s) for the difference.

Fluorescence emission intensity is not in itself a direct measure of binding stoichiometry (*39*). Intensity values are converted to molar units by measuring the fluorescence of the ligand fully bound to the receptor. In most cases, these values can be determined by examining the fluorescence emission spectrum of the ligand in the presence of a large

[2] The stoichiometry of N-AB-PT binding to GTP−tubulin microtubules is slightly greater than 1 mol of ligand/mol of assembled tubulin. This value is treated as 1.0 in the text. An explanation for the discrepancy is found at the end of the Discussion.

[3] A previous study of paclitaxel binding to microtubules found that the apparent affinity of paclitaxel for microtubules was dependent on paclitaxel concentration (*5*, *40*). K_d values of 50 nM and 1 μM for the two types of paclitaxel binding sites were estimated; our K_d values for N-AB-PT binding to GTP−tubulin microtubules are in good agreement with these results.

excess of receptor. The implicit assumption in these analyses is that the emission intensity is directly proportional to the occupancy of the receptor site. We have found, however, that the photochemical lifetime and emission intensity of microtubule-bound N-AB-PT differ by up to 30% depending on the nucleotide content of the polymer (see Results). These differences do not matter in the homogeneous polymer in GMPCPP-tubulin and GDP-tubulin microtubules. GTP-tubulin polymers, though, contain the fluorophore bound in two different environments (i.e., GDP-tubulin-like and GMPCPP-tubulin-like). Thus, it is not possible to determine a priori which fraction of the fluorescent signal is due to the GDP-tubulin-like environment and which type is due to the GMPCPP-tubulin-like environment. The absolute stoichiometry of N-AB-PT bound to GTP-tubulin microtubules therefore cannot be determined with the same accuracy as the stoichiometry of N-AB-PT bound to GDP- or GMPCPP-tubulin microtubules by this spectroscopic method.

CONCLUSIONS

The affinity of tubulin for paclitaxel is highly dependent on its conformation. Unassembled, GTP-tubulin either does not bind paclitaxel or binds the drug with very low affinity (*15*). Assembled tubulin has a high affinity for paclitaxel prior to GTP hydrolysis, which decreases sharply after nucleotide hydrolysis. These results may explain why paclitaxel suppresses dynamic instability at low drug concentrations: the drug binds preferentially to the *end* of the microtubule because it has an intrinsically higher affinity for the conformational state of tubulin found on the microtubule end.[3] It will be interesting to discover whether the cryptophycin binding site or binding sites of other anti-microtubule drugs are equally affected by the nucleotide-engendered conformational state of the protein.

ACKNOWLEDGMENT

We thank Professor John J. Correia for assistance in preparing GMPCPP, Dr. Barbara M. Poliks and Mr. Henry Eichelberger for performing the electron microscopy, Professors Robley C. Williams, Jr., and Jose M. Andreu for helpful discussions, and P & N Packing for providing bovine brains.

REFERENCES

1. Wani, M. C., Taylor, H. L., Wall, M. E., Coggon, P., and McPhail, A. T. (1971) *J. Am. Chem. Soc. 93*, 2325−2327.
2. Rowinsky, E. K. (1997) *Annu. Rev. Med. 48*, 353−374.
3. Wiseman, L. R., and Spencer, C. M. (1998) *Drugs Aging 12*, 305−334.
4. Horwitz, S. B. (1994) *Ann. Oncol. 5, Suppl. 6*, S3−6.
5. Derry, W. B., Wilson, L., and Jordan, M. A. (1995) *Biochemistry 34*, 2203−2211.
6. Suffness, M., and Wall, M. E. (1995) Discovery and Development of Taxol. in *Taxol: Science and applications* (Suffness, M., Ed.) pp 3−25, CRC Press, Inc., Boca Raton, FL.
7. Schiff, P. B., Fant, J., and Horwitz, S. B. (1979) *Nature 277*, 665−667.
8. Scatena, C. D., Stewart, Z. A., Mays, D., Tang, L. J., Keefer, C. J., Leach, S. D., and Pietenpol, J. A. (1998) *J. Biol. Chem. 273*, 30777−30784.
9. Rodi, D. J., Janes, R. W., Sanganee, H. J., Holton, R. A., Wallance, B. A., and Makowski, L. (1999) *J. Mol. Biol. 285*, 197−203.
10. Schimming, R., Mason, K. A., Hunter, N., Weil, M., Kishi, K., and Milas, L (1999) *Cancer Chemother. Pharmacol. 43*, 165−172.
11. Torres, K., and Horwitz, S. B. (1998) *Cancer Res. 58*, 3620−3626.
12. Toso, R. J., Jordan, M. A., Farrel, K. W., Matsumoto, B., and Wilson, L. (1993) *Biochemistry 32*, 1285−1293.
13. Panda, D., Himes, R. H., Moore, R. E., Wilson L., and Jordan, M. A. (1997) *Biochemistry 36*, 12948−12953.
14. Diaz, J. F., and Andreu, J. M. (1993) *Biochemistry 32*, 2747−2755.
15. Sengupta, S., Boge, T. C., Georg, G. I., and Himes, R. (1995) *Biochemistry 34*, 11889−11894.
16. Diaz, J., Menendez, M., and Andreu, J. M. (1993) *Biochemistry 32*, 10067−10077.
17. Caplow, M., Shanks, J., and Ruhlen, R. (1994) *J. Biol. Chem. 269*, 23399−23402.
18. Han, Y., Chaudhary, A. G., Chordia, M. D., Sackett, D. L., Perez-Ramirez, B., Kingston, D. G., and Bane, S. (1996) *Biochemistry 35*, 14173−14183.
19. Li, Y., Poliks, B., Cegelski, L., Poliks, M., Gryczynski, Z., Piszczek, G., Jagtap, P. G., Studelska, D., Kingston, D. G. I., Schafer, J., and Bane, S. (1999) *Biochemistry 36* (in press).
20. Kingston, D. G., Chaudhary, A. G., Chordia, M. D., Gharpure, M., Gunatilaka, A. A., Higgs, P. I., Rimoldi, J. M., Samala, L., Jagtap, P. G., Giannakakou, P., Jiang, Y. Q., Lin, C. M., Hamel, E., Long, B. H., Fairchild, C. R., and Johnston, K. A. (1998) *J. Med. Chem. 41*, 3715−3726.
21. Vulevic, B., and Correia, J. J. (1997) *Biophys. J. 72*, 1357−1375.
22. Williams, R. C., Jr., and Lee, J. C. (1982) *Methods Enzymol. 85*, 376−385.
23. Detrich, H. W., III, and Williams, R. C., Jr. (1978) *Biochemistry 17*, 3900−3907.
24. Dye, R. B., and Williams, R. C., Jr. (1996) *Biochemistry 35*, 14331−14339.
25. Seckler, R., Wu, G. M., and Timasheff, S. N. (1990) *J. Biol. Chem. 265*, 7655−7661.
26. Hyman, A. A., Salser, S., Drechsel, D. N., Unwin, N., and Mitchison, T. J. (1992) *Mol. Biol. Cell 3*, 1155−1167.
27. Lakowicz, J. R. (1983) *Principles of Fluorescence Spectroscopy*, pp 74−84, Plenum Press, New York.
28. Vandecandelaere, A., Martin, S. R., and Bayley, P. M. (1995) *Biochemistry 34*, 1332−1343.
29. Diaz, J. F., Valpuesta, J. M., Chacon, P., Diakun, G., and Andreu, J. M. (1998) *J. Biol. Chem. 273*, 33803−33810.
30. Hyman, A. A., Chretien, D., Arnal, I., and Wade, R. H. (1995) *J. Cell Biol. 128*, 117−125.
31. Müller-Reichert, T., Chretien, D., Severin, F., and Hyman, A. A. (1998) *Proc. Natl. Acad. Sci. U.S.A. 95*, 3661−3666.
32. Howard, W. D., and Timasheff, S. N. (1986) *Biochemistry 25*, 8292−8300.
33. Correia, J. J. (1991) *Pharmacol. Ther. 52*, 127−147.
34. Babier, P., Peyrot, V., Leynadier, D., and Andreu, J. M. (1998) *Biochemistry 37*, 758−768.
35. Parness, J., and Horwitz, S. B. (1981) *J. Cell Biol. 91*, 479−487.
36. Carlier, M. F., and Pantaloni, D. (1983) *Biochemistry 22*, 4814−4822.
37. Wilson, L., Miller, H. P., Farrell, K. W., Snyder, K. B., Thompson, W. C., and Purich, D. L. (1985) *Biochemistry 24*, 5254−5262.
38. Arnal, I., and Wade, R. H. (1995) *Curr. Biol. 5*, 900−908.
39. Timasheff, S. N., Andreu, J. M., and Na, G. C. (1991) *Pharmacol. Ther. 52*, 191−210.
40. Derry, W. B. (1996) *The Molecular Mechanism of Action of the Anticancer Drug Taxol: Substoichiometric Suppression of Microtubule Dynamics and the Role of Beta Tubulin Isotypes in Resistance*, Dissertation, University of California at Santa Barbara, pp 26−54.

BI992044U